Analysis of Protein Mixtures by Electrospray Mass Spectrometry: Effects of Conformation and Desolvation Behavior on the Signal Intensities of Hemoglobin Subunits

Mark C. Kuprowski, Brian L. Boys, and Lars Konermann
Department of Chemistry, The University of Western Ontario, London, Ontario, Canada

The determination of solution-phase protein concentration ratios based on ESI-MS intensity ratios is not always straightforward. For example, equimolar mixtures of hemoglobin α- and β-subunits consistently result in much higher peak intensities for the α-chain. The current work explores the origin of this effect. Under mildly acidic conditions (pH 3.4) α-globin is extensively unfolded, whereas β-globin retains residual structure. Because of its greater nonpolar character, the more unfolded α-subunit can more effectively compete for charge. This leads to suppression of β-globin signals under conditions where the protein ion yield is limited by the charge concentration on the initially formed ESI droplets. More balanced intensities are observed when operating under charge excess conditions and/or in a solvent environment where both proteins are unfolded to a similar degree (pH 2.2). However, even in these cases the overall α-globin peak intensity is still twice as high as that of the β-subunit. The persistent imbalance under these conditions originates from the different declustering behaviors of the two proteins. A considerable fraction of β-globin undergoes incomplete desolvation during ESI, thereby reducing the intensity of bare $[\beta + z\mathrm{H}]^{z+}$ ions. When including the contributions of incompletely desolvated species, the overall α:β ion intensity ratio is close to unity. The α:β intensity imbalance can also be eliminated by a strongly elevated declustering potential in the ion sampling interface. In conclusion, important factors that have to be considered for the ESI-MS analysis of protein mixtures are (1) conformational effects, resulting in differential surface activities, and (2) dissimilarities in the protein desolvation behavior. (J Am Soc Mass Spectrom 2007, 18, 1279–1285) © 2007 American Society for Mass Spectrometry

Electrospray ionization mass spectrometry (ESI-MS) has become an important tool for characterizing the biochemical and biophysical properties of proteins [1]. Different polypeptide chains in solution can be distinguished based on their mass, their ligand-binding behavior [2, 3], their hydrogen–deuterium exchange (HDX) properties [4–7], and their charge state distributions [8–11]. Unfolded conformations generally result in higher ESI charge states than tightly folded structures, an effect that mirrors the lower compactness and the larger solvent-accessible surface area of the unfolded state [12, 13]. The combination of these features results in an unsurpassed selectivity that greatly facilitates the detection of coexisting species. One problem, however, that can complicate the analysis of ESI-MS data is that the measured ion intensities do not necessarily reflect the relative concentrations of the corresponding proteins in solution [14]. The apparent ionization efficiencies of different biomacromolecules can vary by several orders of magnitude [15]. The situation is further complicated by ion-suppression effects that may occur in protein mixtures and in the presence of other solutes [16–19]. An improved understanding of the relationship between ESI-MS signal response and solution-phase concentration would be beneficial for a wide range of applications.

The upper limit of the ionization efficiency in ESI-MS is determined by the molar concentration of excess charge, C_q, on the initially formed electrospray droplets [19, 20]. C_q can be estimated based on the relationship

$$C_q \approx \frac{4.2}{F}\left[\frac{K\gamma}{V_f \kappa_e}\right]^{1/2}$$

where K is the conductivity of the solution, γ is the surface tension of the solvent, V_f is the solvent flow rate, κ_e is the dielectric constant, and $F = 96{,}485$ C mol^{-1} [19]. When analyzing a mixture containing n different protein species, the molar concentration of charge C_0 that would be required for the ionization of *all* proteins is

$$C_0 \approx \sum_{i=1}^{n} C_i \times \bar{q}_i$$

where C_i and $\bar{q}_i$ are the concentration and the average

Address reprint requests to Dr. Lars Konermann, Department of Chemistry, The University of Western Ontario, London, ON, N6A 5B7, Canada. E-mail: konerman@uwo.ca

1044-0305/07/$32.00
doi:10.1016/j.jasms.2007.04.002

Published online April 15, 2007
Received February 13, 2007
Revised March 31, 2007
Accepted April 5, 2007

charge state, respectively, of protein *i*. Accordingly, two regimes can be distinguished [21]. Under charge deficient conditions ($C_q < C_0$) only a fraction of the proteins in the sample can be ionized. The analyte that competes most effectively for the available charge on the droplet surface will show the highest relative signals, thereby suppressing the ionization of other species [22–24]. On the other hand, charge excess ($C_q > C_0$) corresponds to a regime where suppression effects are much less pronounced. From eqs 1 and 2 it follows that the latter condition can be promoted by using low analyte concentrations and low flow rates [22, 25].

The native conformation of water-soluble globular proteins generally exhibits a hydrophobic core consisting of nonpolar residues, whereas most hydrophilic side chains are located on the outside where they can interact with the solvent. Unfolding exposes a large number of hydrophobic residues, thereby increasing the nonpolar character of the protein. Our laboratory recently proposed a simple framework to account for the occurrence of suppression effects in mixtures containing coexisting protein conformers [21]. We noted that unfolded polypeptide chains tend to result in a much stronger ESI-MS signal response than native proteins. The higher ionization efficiency of unfolded proteins was attributed to their partially nonpolar character that provides an enhanced surface activity. An increased affinity for the air–liquid interface facilitates the transfer of unfolded proteins into progeny droplets that are generated from the surface layers of the parent droplet. Because it is these small and highly charged progeny droplets that ultimately release analyte ions into the gas phase, unfolded proteins tend to show higher ionization efficiencies [26–28]. Conversely, natively folded proteins have a lower affinity for the air–liquid interface. Thus, these species tend to stay behind in the charge-depleted residual parent droplet, such that their ionization is suppressed. This proposed scenario [21], where unfolded proteins compete most effectively for charge on the droplet surface arising from their increased hydrophobicity is consistent with numerous mechanistic studies on the ESI process [15, 29–33]. We demonstrated that differences in the ionization efficiency between native and unfolded conformers are very pronounced in the charge-deficient regime. In contrast, suppression effects were minimized under charge-surplus conditions [21].

The current work extends our previous findings by focusing on a particularly interesting phenomenon. Native hemoglobin (Hb) is a $(\alpha\beta)_2$ heterotetramer where each of the subunits carries a heme group. Hb is among the most thoroughly studied protein complexes [34] and it has been the subject of a considerable number of ESI-MS–based investigations [11, 35–43]. Exposure of the protein to acidic conditions induces the disassembly of the native quaternary structure, disruption of the heme–protein interactions, and extensive unfolding of the individual subunits [36]. ESI-MS and nanoESI-MS experiments on acid-denatured Hb consistently reveal a strongly imbalanced α:β ion intensity ratio, with considerably higher signals for α-globin [36–39, 43]. Apparently the origin of this behavior has not been thoroughly explored yet. Our results reveal that in addition to charge availability and protein conformation, a major factor responsible for the observed imbalance is the different desolvation behaviors of the two subunits. Apparently the conclusions reached here for Hb should apply to other protein mixtures as well.

Experimental

Materials

Bovine ferri-Hb was purchased from Sigma (St. Louis, MO, USA). Ammonium acetate and formic acid (98%) were bought from Fluka (Buchs, Switzerland). Hb stock solutions (~200 μM, as tetramer) were prepared by dissolving the protein in 10 mM aqueous ammonium acetate. A small amount of insoluble debris was removed by centrifugation. The supernatant was dialyzed against 10 mM ammonium acetate using a Slide-A-Lyzer cassette (Pierce, Rockford, IL, USA) with a nominal 7 kDa molecular weight cutoff. Post dialysis, samples were flash frozen in liquid nitrogen and stored at −80 °C. Before analysis, the stock solution was diluted to the desired tetramer concentration (0.4 or 40 μM) using 10 mM ammonium acetate. Protein concentrations of native Hb were determined by UV-Vis spectrophotometry, based on an absorption coefficient of ε_{280} = 111,060 M^{-1} cm^{-1} for the tetramer. This value takes into account protein and heme contributions to the molar absorptivity [44]. The solution pH was adjusted with formic acid. Deuterium oxide was obtained from Cambridge Isotope Laboratories (Andover, MA, USA). pH and pD values were measured with an AB15 pH meter (Fisher Scientific, Nepean, Ontario, Canada). Reported values for D_2O-containing solutions were corrected for isotope effects by using the relation pD = pH meter reading + 0.4 [45].

Liquid Chromatography

HPLC experiments were carried out using a mobile phase consisting of glass-distilled acetonitrile (Caledon Laboratories, Georgetown, Ontario, Canada) and water, both with 0.05% trifluoroacetic acid (Sigma), resulting in pH 2.2. α- and β-subunits were separated on a Waters Symmetry 300 (Milford, MA, USA), C4 3.5 μm, 2.1 × 100 mm column, using a shallow linear organic gradient at a flow rate of 100 μL min^{-1}. The concentration and volume of individual Hb injections were 4 μM and 10 μL, respectively. Average monomer concentrations across individual peaks in the chromatogram were about 0.4 μM. For optical LC runs, a 2695 HPLC pump was coupled to a photodiode array detector (model 996, Waters, Manchester, UK). The absorption coefficients of the heme-free subunits at 280 nm were determined using the ExPASy web server, resulting in values of 9970 and 13,980 M^{-1} cm^{-1} for α and β, respectively. LC-MS experiments were carried out using a 1525μ HPLC pump (Waters) under otherwise identical conditions.

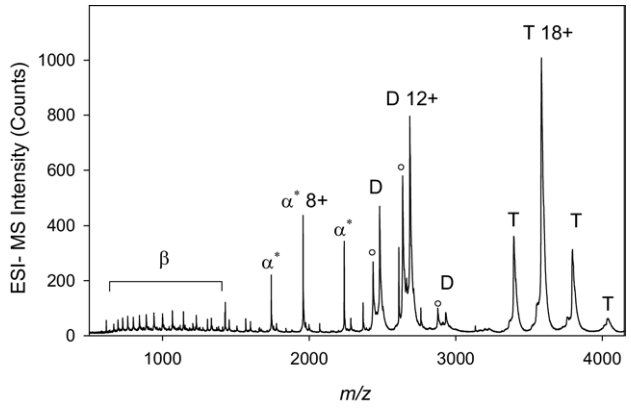

Figure 1. ESI mass spectrum of 50 μM Hb in 10 mM ammonium acetate at pH 6.8. Ions corresponding to the intact (holo-α holo-β)$_2$ tetramer are labeled as *T* (holo-α holo-β); dimers are labeled as *D*. Open circles correspond to heme-deficient dimers (holo-α apo-β). Peaks marked as α^* and β represent monomeric holo-α and apo-β subunits, respectively. Also indicated are the charge states of a few selected ions.

Mass Spectrometry

Unless noted otherwise, ESI mass spectra were recorded on a Q-TOF Ultima API equipped with a Z-spray source (Waters), operated in positive ion mode at a capillary voltage of 3.0 kV. The spectra were found to be insensitive to changes in cone voltage between 0 and 35 V. Cone and desolvation gas flow rates were 50 and 500 L h^{-1}, respectively. Measurements were carried out using a desolvation temperature of 120 °C and a source temperature of 80 °C. All spectra were acquired with an integration time of 10 s and represent the average of at least 15 scans.

Hydrogen–Deuterium Exchange

On-line HDX was initiated by exposing 4 μM Hb to a 95:5 (vol/vol) D_2O/H_2O mixture that contained 25 μM bradykinin (RPPGFSPFR, Bachem Bioscience Inc., King of Prussia, PA, USA) as internal standard. The pD of this labeling solution was adjusted with formic acid to 3.4 or 2.2. The mixture was infused on-line into the ion source of the mass spectrometer at a flow rate of 5 μL min^{-1} using a syringe pump (Harvard Apparatus, South Natick, MA, USA). The relative HDX level of bradykinin was calculated as described previously [46]. Relative HDX levels for the Hb α- and β-subunits were determined by dividing the measured mass shift ΔM by the number of exchangeable hydrogen atoms: 228 for α and 245 for β. ΔM values were determined as average from the three most intense peaks in the spectra by converting the mass-to-charge ratio values of the original data according to $\Delta M = (r \times z) - m_{charge} - M_0$, where r is the mass-to-charge ratio, z is the charge state of the ion, m_{charge} is the combined mass of the z charge carriers (protons and deuterons, their numbers being determined by the D_2O to H_2O ratio in solution), and M_0 is the mass of the unlabeled protein, 15,053 and 15,954 Da for the apo-α and apo-β chains, respectively [42].

Results and Discussion

At near-neutral pH the ESI mass spectrum of Hb is dominated by ions corresponding to the intact tetrameric quaternary structure. In addition, dimeric species as well as minor contributions from monomeric holo-α and apo-β ions are observed (Figure 1). These data are consistent with previous ESI-MS spectra recorded under native solvent conditions [11, 35–37, 40]. Isotope labeling studies have shown that nontetrameric ions in the spectrum reflect the presence of the corresponding species in solution, that is, dimers and monomers are not products of fragmentation processes during ESI [38].

Acidification to pH 3.4 induces protein denaturation and results in the formation of heme-free monomeric α- and β-chains [36] (Figure 2). The high charge states of the observed protein ions show that both apo subunits adopt considerably unfolded solution-phase conformations [8–11]. The spectrum in Figure 2a, recorded at a protein concentration of 80 μM for each of the subunits, exhibits dramatically lower signal intensities for the β-subunit than for α. The overall α:β peak intensity ratio is 8.4. A stoichiometric excess of α-globin in the sample would provide a trivial explanation for the observed effect. However, this scenario seems unlikely, considering that the spectrum of native Hb (Figure 1) is dominated by $(\alpha\beta)_2$ tetramers and $\alpha\beta$ dimers, thereby suggesting an α:β concentration ratio close to unity. The stoichiometric ratio in solution was measured directly by UV-Vis absorption spectroscopy after separating the subunits by HPLC under acidic conditions, resulting in

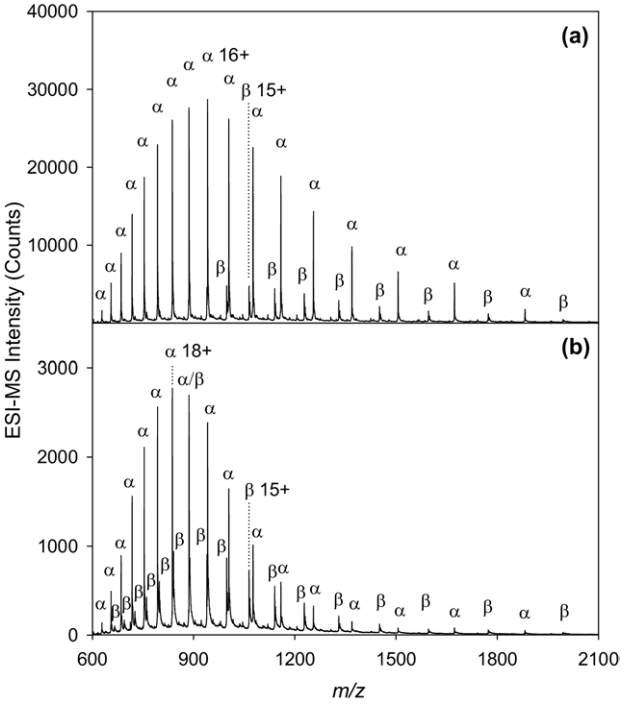

Figure 2. ESI mass spectra of Hb at pH 3.4, using a concentration of (**a**) 80 μM and (**b**) 0.8 μM for each of the subunits. The spectra were recorded by direct infusion using a flow rate of 1 μL min^{-1}.

a value of 1.0 ± 0.1 (data not shown). Thus, it can be ruled out that the higher ESI-MS response of α-globin is caused by simple concentration effects.

It is instructive to consider the concentration of excess charge, C_q, that is available under the conditions of Figure 2a. With $K = 0.25\ S\ m^{-1}$ [19, 22], $\gamma = 0.07\ N\ m^{-1}$, $\kappa_e = 80$, and $V_f = 1\ \mu L\ min^{-1}$ it follows from eq 1 that $C_q \approx 160\ \mu M$. For the spectrum in Figure 2a the average charge states are $\bar{q}_\alpha = 16+$ and $\bar{q}_\beta = 14+$. With a protein concentration of 80 μM for each subunit the concentration of charge required for the ionization of all the proteins in the sample is $C_0 = 2400\ \mu M$ (eq 2). Thus, the data in Figure 2a represent conditions of severe charge deficiency ($C_q \ll C_0$). As outlined in the Introduction, such a scenario will result in suppression of the species with the lower surface activity [21]. Thus, the observed signal intensity ratio suggests that α-globin can compete for charge more effectively than the β-subunit under the conditions used here. Keeping in mind the results of previous studies [15, 21, 29–32], this implies that β-globin has a less nonpolar character, which results in a reduced surface activity. A sequence analysis reveals that differences in the overall hydrophobicity of the two subunits cannot be directly attributed to their amino acid composition. When assigning Kyte–Doolittle scores to every residue, ranging from 4.5 for Ile to −4.5 for Arg [47], it is found that the average hydrophobicities of the α- and β-globin sequences are virtually identical, 0.017 and 0.020, respectively. This suggests that the differences in nonpolar character must be linked to conformational effects.

HDX measurements were carried to probe possible structural differences under the conditions of Figure 2. The HDX kinetics of proteins is highly sensitive to their overall structure; unfolded conformations undergo HDX at higher rates than species that are more folded [48, 49]. Although primary structure effects are also known to affect these rates, this factor is negligible for the HDX properties of the two globin subunits [50]. Instead, differences in the isotope exchange kinetics must be attributed to the degree by which exchangeable sites are protected, either sterically or through hydrogen bonding. It is found that the HDX behavior of α-globin at pD 3.4 is very similar to that of the unstructured control peptide bradykinin, implying that this protein is extensively unfolded and, therefore, has most of its hydrophobic residues exposed to the solvent (Figure 3) [51]. In contrast, β-globin shows notably slower exchange kinetics, thereby proving that the β-subunit retains more folded structure at pH 3.4 than α-globin. Because partially folded proteins typically exhibit a hydrophobic core, it can be inferred that β-globin has at least some nonpolar residues shielded from the solvent under the conditions of this experiment [52]. These findings support the conclusion reached earlier—that the greater degree of unfolding of the α-subunit and the concomitant exposure of nonpolar residues results in a greater surface activity than for β-globin.

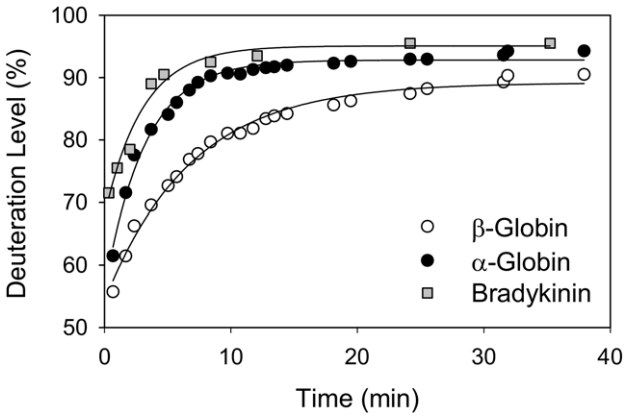

Figure 3. Mass shifts of α- and β-globin measured after incubation of the two proteins in 95% D_2O, 5% H_2O at pD 3.4. Also shown are the HDX kinetics of the unstructured peptide bradykinin for comparison. Solid lines are exponential fits of the form: Deuteration Level = $y_0 + a(1 - e^{-kt})$, with $y_0 = 56$, $a = 37$, and $k = 0.31\ min^{-1}$ for α-globin; $y_0 = 54$, $a = 35$, and $k = 0.15\ min^{-1}$ for β-globin.

For the spectrum in Figure 2b the protein concentration was reduced to 0.8 μM for each subunit, while leaving the other experimental conditions identical to those of Figure 2a. With $\bar{q}_\alpha = \bar{q}_\beta = 18+$ the data of Figure 2b represent a charge-surplus scenario ($C_q > C_0$) because $C_0 \approx 29\ \mu M$ and $C_q \approx 160\ \mu M$. This charge surplus induces a noticeable shift of the spectrum to higher protonation states when compared to Figure 2a [20, 21]. Importantly, signal suppression under these conditions is not as pronounced. The relative intensity of β-globin increases almost fourfold, resulting in an α:β peak intensity ratio of 2.4. However, even in Figure 2a the β-globin intensities remain notably lower than those of the α-subunit. This persistent imbalance is surprising, considering that the available charge should be sufficient to eliminate suppression effects, regardless of the structure and surface activity of the proteins involved [21].

To gain further insights into the role of conformational effects, ESI mass spectra were recorded under more acidic conditions (pH 2.2) that promote further unfolding of β-globin (Figure 4). HDX measurements confirm that the degree of unfolding for the α- and β-chains is more similar at pD 2.2 than at pD 3.4 (Figure 5). Both proteins appear to retain little residual structure, reaching a final HDX level close to 95% after 20 min. However, small differences in the isotope exchange behavior persist. ESI mass spectra recorded at monomer concentrations of 80 μM (Figure 4a) and 0.8 μM (Figure 4b) once again represent conditions of charge deficiency and charge surplus, respectively. Interestingly, the α:β intensity ratios observed in both experiments are virtually identical, with values of 2.2 and 1.9. Very similar spectra and HDX kinetics were recorded when the pH was lowered even further to 1.5 (data not shown). The observation that the relative α and β ion intensities are independent of the C_q:C_0 ratio strongly suggests that both subunits exhibit almost the

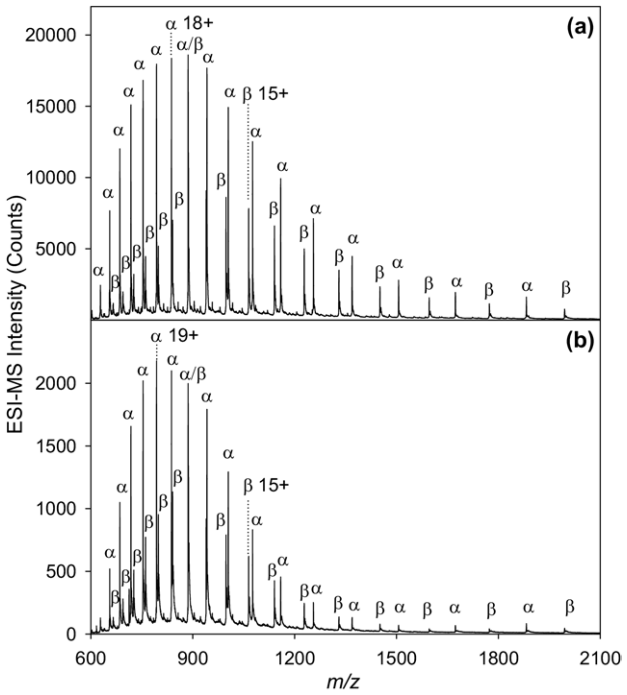

Figure 4. ESI mass spectra of Hb at pH 2.2, using a concentration of (**a**) 80 μM and (**b**) 0.8 μM for each of the subunits. The spectra were recorded by direct infusion using a flow rate of 1 μL min^{-1}.

same surface activities at pH 2.2, a result that is consistent with the HDX data in Figure 5. It is unexpected, however, that the signal intensity of α-globin under these conditions still remains significantly higher than that of β-globin. This leads us to conclude that surface activities and the availability of charge are not the only factors that need to be considered to account for the observed imbalance.

Clues to the origin of the consistently biased α:β intensity ratio come from LC-MS analyses of the globin mixture at pH 2.2. Suppression effects should be absent in these experiments as a result of the spatial and temporal separation of the two proteins. Integration of

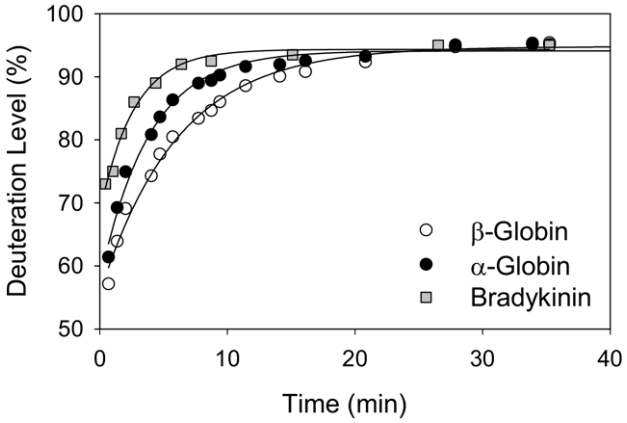

Figure 5. HDX kinetics α- and β-globin as in Figure 3, but at pD 2.2. Fitting parameters: y_0 = 58, a = 37, and k = 0.26 min^{-1} for α-globin; y_0 = 56, a = 39, and k = 0.16 min^{-1} for β-globin.

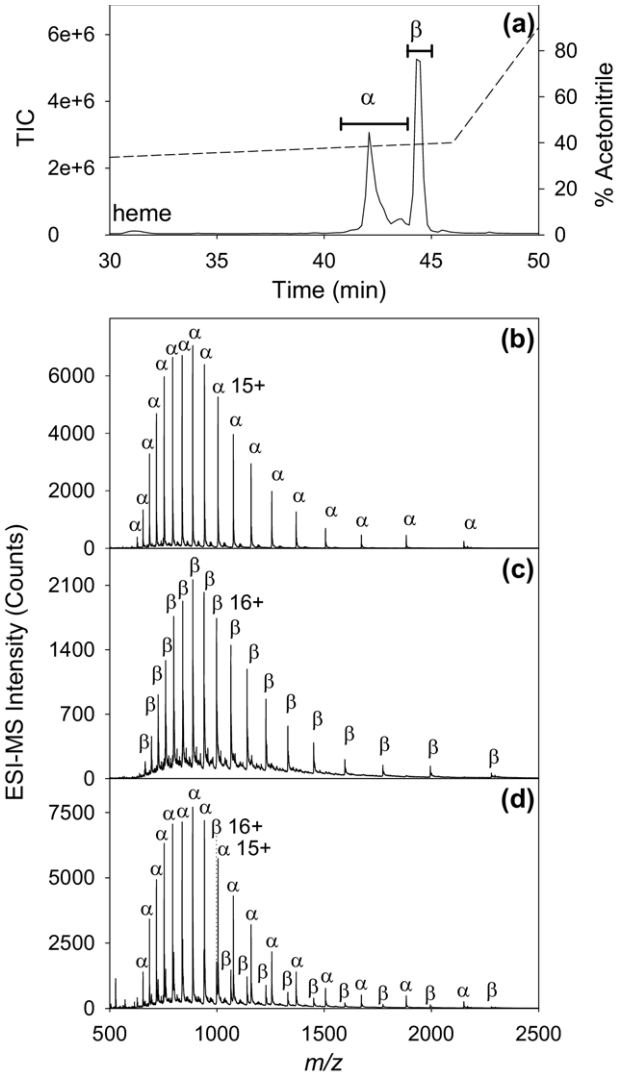

Figure 6. Separation of Hb subunits by HPLC/ESI-MS. (**a**) TIC trace, indicating signals that correspond to heme, α- and β-globin. The small signal at t = 44 min is attributed to α+16 and α+32 species, possibly oxidation artifacts generated during ESI. The acetonitrile gradient used is shown as a dashed line. (**b**), (**c**) spectra of α- and β-globin, obtained by integrating the TIC sections indicated in the top panel. (**d**) Spectrum extracted from the integrated TIC between t = 40 and t = 45 min.

the α- and β-globin total ion current (TIC) sections results in a peak area ratio of 0.9, that is, close to unity (Figure 6a). This ratio, however, appears to be at odds with the ESI-MS spectra extracted from the two regions that, once again, show *lower* peak intensities for the β-subunit (Figure 6b, c). Similarly, the spectrum obtained from the combined TIC sections of the two subunits is strongly dominated by α-globin peaks (Figure 6d). This apparent contradiction is resolved by noting that most of the β-globin TIC is caused by a strongly elevated baseline (Figure 6c), whereas the TIC of the α-subunit is dominated by bare $[\alpha + z\mathrm{H}]^{z+}$ ions (Figure 6b). We attribute the chemical noise underlying the peaks of the β-subunit to the presence of incompletely desolvated β-globin ions [53, 54]. Thus, a major

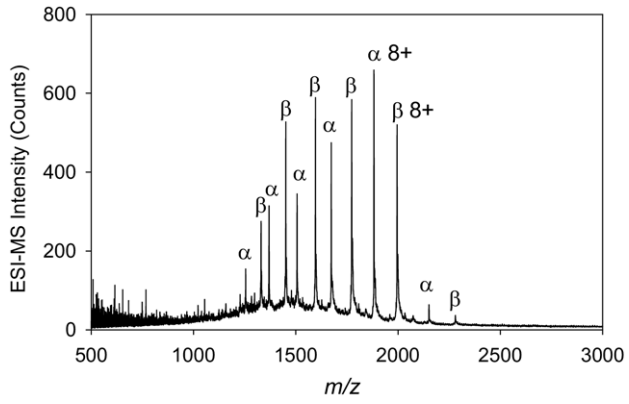

Figure 7. ESI mass spectrum of 4 μM Hb at pH 2.2 recorded under "harsh" conditions on a Waters LCT instrument equipped with a Z-spray source. The declustering potential (cone voltage) was increased to 85 V. In addition, the source speedy valve was fully open, which lowers the pressure in the hexapole ion guide and further increases the "harshness" of the ion sampling process [59].

factor contributing to the persistently low β-globin signal intensities is the fact that a considerable proportion of the protein ions remains bound to low molecular weight species, likely solvent molecules. This results in a spread of the overall ion intensity over a relatively wide m/z range, thereby reducing the abundance of properly declustered $[\beta + zH]^{z+}$ ions.

Support for this interpretation comes from experiments on a globin mixture at pH 2.2 carried out with an elevated declustering potential (cone voltage). These conditions facilitate the complete desolvation of gas-phase proteins in the ion sampling interface. Data obtained in this way exhibit relatively balanced intensities for the two subunits, with an α:β peak intensity ratio of 0.8 (Figure 7). The observation that the intensity bias favoring α-globin ions can be eliminated in this way underpins the notion that differences in the desolvation behavior are an important aspect for the imbalanced α:β intensity ratios under regular (soft) ESI conditions. Analogous observations were made by Frahm et al. [55], who demonstrated that thermal activation in the ion sampling interface resulted in a leveling of the ESI-MS response for various DNA strands. The shift of the spectrum in Figure 7 to lower charge states is attributable to collision-induced dissociation (CID), a process that preferentially affects highly charged ions as a result of their increased electrostatic and kinetic energy. The α- and β-globin CID fragments generated in this way are responsible for the significant chemical noise in the spectrum [53].

Conclusions

The goal of this study was to elucidate why some proteins in a mixture consistently show higher ESI-MS intensities than others. In agreement with earlier work [21] it is found that the ability of a protein to compete for charge is strongly affected by its solution-phase conformation. Proteins that are highly denatured and expose their nonpolar residues to the solvent show a higher surface activity than that of species that retain a more folded structure. This situation applies to the data in Figure 2, where β-globin retains a more folded conformation than does α-globin. If the overall protein yield is limited by the available charge ($C_q < C_0$), such a conformational difference results in a severe suppression of the more folded protein (Figure 2a) [15, 21, 29, 31, 32]. Imbalances in ionization efficiency that originate from differential surface activities can be greatly reduced by working under conditions of charge excess ($C_q > C_0$). This explains why the suppression of β-globin is less pronounced in Figure 2b than in Figure 2a. In cases where two proteins exhibit comparable surface activities, their signal intensity ratio is virtually unaffected by the degree to which charge is available (Figure 4). However, another important factor that has to be taken into account concerns differences in the desolvation behavior. Incomplete desolvation leads to a spread of the overall ion intensity, thereby elevating the baseline background and reducing the intensity of bare $[M + zH]^{z+}$ ions. For the Hb system investigated here desolvation effects greatly contribute to a consistently biased α:β peak intensity ratio. Unfortunately, the experiments described here cannot elucidate the reasons that are ultimately responsible for the poor desolvation properties of the β-chain. It is hoped that future studies on the hydration behavior of biomolecules in the gas phase will provide further insights into this interesting question [56]. Collisional activation in the ion sampling interface leads to a leveling of the signals originating from differentially desolvated proteins, an effect that was previously observed for other types of analytes [55].

From the results of this work we conclude that one has to be careful when estimating concentration ratios of proteins in solution based on ESI-MS peak intensities, an issue that is of particular relevance for the determination of protein–ligand binding affinities [57, 58]. Depending on the experimental conditions, substantial deviations can occur. The extent of these deviations is affected by the conformations and the resulting surface activities of the various polypeptide chains, the magnitude of C_q relative to C_0, and the desolvation behavior of the proteins during ESI. To ensure that ESI-MS data most accurately reflect solution-phase concentration ratios it is important that the experiments are carried out in the charge-excess regime and under conditions favoring complete desolvation.

Acknowledgments

This work was supported by the Natural Sciences and Engineering Research Council of Canada (NSERC), the Canada Foundation for Innovation (CFI), and the Canada Research Chairs Program. HPLC experiments with UV detection were carried out at the UWO-BIC Facility.

References

1. Fenn, J. B. Electrospray Wings for Molecular Elephants (Nobel Lecture). *Angew. Chem. Int. Ed.* **2003**, *42*, 3871–3894.
2. Loo, J. A. Noncovalent protein–ligand complexes. In: *The Encyclopedia of Mass Spectrometry*, Gross, M. L.; Caprioli, R. M., Eds.; Elsevier: Amsterdam, 2005; vol. 2, pp 289–299.
3. Heck, A. J. R.; Van den Heuvel, R. H. H. Investigation of Intact Protein Complexes by Mass Spectrometry. *Mass Spectrom. Rev.* **2004**, *23*, 368–389.
4. Wales, T. E.; Engen, J. R. Hydrogen Exchange Mass Spectrometry for the Analysis of Protein Dynamics. *Mass Spectrom. Rev.* **2006**, *25*, 158–170.
5. Kaltashov, I. A.; Engen, J. R.; Gross, M. L. Hydrogen Exchange and Covalent Modification: Focus on Biomolecular Structure, Dynamics, and Function. 18th Sanibel Conference on Mass Spectrometry. *J. Am. Soc. Mass Spectrom.* **2006**, *17*, i–ii.
6. Konermann, L.; Simmons, D. A. Protein Folding Kinetics and Mechanisms Studied by Pulse-Labeling and Mass Spectrometry. *Mass Spectrom. Rev.* **2003**, *22*, 1–26.
7. Chik, J. K.; Schriemer, D. C. Hydrogen/Deuterium Exchange Mass Spectrometry of Actin in Various Biochemical Contexts. *J. Mol. Biol.* **2003**, *334*, 373–385.
8. Chowdhury, S. K.; Katta, V.; Chait, B. T. Probing Conformational Changes in Proteins by Mass Spectrometry. *J. Am. Chem. Soc.* **1990**, *112*, 9012–9013.
9. Invernizzi, G.; Samalikova, M.; Brocca, S.; Lotti, M.; Molinari, H.; Grandori, R. Comparison of Bovine and Porcine β-Lactoglobulin: A Mass Spectrometric Analysis. *J. Mass Spectrom.* **2006**, *41*, 717–727.
10. Eyles, S. J.; Kaltashov, I. A. Methods to Study Protein Dynamics and Folding by Mass Spectrometry. *Methods* **2004**, *34*, 88–99.
11. Boys, B. L.; Konermann, L. Folding and Assembly of Hemoglobin Monitored by Electrospray Mass Spectrometry Using an On-line Dialysis System. *J. Am. Soc. Mass Spectrom.* **2007**, *18*, 8–16.
12. de la Mora, F. J. Electrospray Ionization of Large Multiply Charged Species Proceeds via Dole's Charged Residue Mechanism. *Anal. Chim. Acta* **2000**, *406*, 93–104.
13. Kaltashov, I. A.; Mohimen, A. Estimates of Protein Surface Area in Solution by Electrospray Ionization Mass Spectrometry. *Anal. Chem.* **2005**, *77*, 5370–5379.
14. Dobo, A.; Kaltashov, I. A. Detection of Multiple Protein Conformational Ensembles in Solution via Deconvolution of Charge-State Distributions in ESI MS. *Anal. Chem.* **2001**, *73*, 4763–4773.
15. Cech, N. B.; Enke, C. G. Practical Implication of Some Recent Studies in Electrospray Ionization Fundamentals. *Mass Spectrom. Rev.* **2001**, *20*, 362–387.
16. Iavarone, A. T.; Udekwu, O. A.; Williams, E. R. Buffer Loading for Counteracting Metal Salt-induced Signal Suppression in Electrospray Ionization. *Anal. Chem.* **2004**, *76*, 3944–3950.
17. Gustavsson, S. A.; Samskog, J.; Karkides, K. E.; Langstrom, B. Studies of Signal Suppression in Liquid Chromatography–Electrospray Ionization Mass Spectrometry Using Volatile Ion-pairing Reagents. *J. Chromatogr. A* **2001**, *937*, 41–47.
18. Xu, N.; Lin, Y.; Hofstadler, S. A.; Matson, D.; Call, C. J.; Smith, R. D. A Microfabricated Dialysis Device for Sample Cleanup in Electrospray Ionization Mass Spectrometry. *Anal. Chem.* **1998**, *70*, 3553–3556.
19. Pan, P.; McLuckey, S. A. Electrospray Ionization of Protein Mixtures at Low pH. *Anal. Chem.* **2003**, *75*, 1491–1499.
20. Wang, G.; Cole, R. Mechanistic Interpretation of the Dependence of Charge State Distributions on Analyte Concentrations in Electrospray Ionization Mass Spectrometry. *Anal. Chem.* **1995**, *67*, 2892–2900.
21. Kuprowski, M. C.; Konermann, L. Signal Response of Co-existing Protein Conformers in Electrospray Mass Spectrometry. *Anal. Chem.* **2007**, *79*, 2499–2596.
22. Schmidt, A.; Karas, M.; Dülcks, T. Effect of Different Solution Flow Rates on Analyte Signals in Nano-ESI MS, or: When Does ESI Turn into Nano-ESI. *J. Am. Soc. Mass Spectrom.* **2003**, *14*, 492–500.
23. Smith, R. D.; Shen, Y.; Tang, K. Ultrasensitive and Quantitative Analyses from Combined Separations–Mass Spectrometry for the Characterization of Proteomes. *Acc. Chem. Res.* **2004**, *37*, 269–278.
24. Tang, K.; Page, J. S.; Smith, R. D. Charge Competition and the Linear Dynamic Range of Detection in Electrospray Ionization Mass Spectrometry. *J. Am. Soc. Mass Spectrom.* **2004**, *15*, 1416–1423.
25. El-Faramawy, A.; Siu, M. K. W.; Thomson, B. A. Efficiency of Nano-Electrospray Ionization. *J. Am. Soc. Mass Spectrom.* **2005**, *16*, 1702–1707.
26. Kebarle, P.; Peschke, M. On the Mechanisms by Which the Charged Droplets Produced by Electrospray Lead to Gas Phase Ions. *Anal. Chim. Acta* **2000**, *406*, 11–35.
27. Duft, D.; Achtzehn, T.; Muller, R.; Huber, B. A.; Leisner, T. Coulomb Fission: Rayleigh Jets from Levitated Microdroplets. *Nature* **2003**, *421*, 128.
28. Gomez, A.; Tang, K. Charge and Fission of Droplets in Electrostatic Sprays. *Phys. Fluids* **1994**, *6*, 404–414.
29. Tang, K.; Smith, R. D. Physical/Chemical Separations in the Break-up of Highly Charged Droplets from Electrosprays. *J. Am. Soc. Mass Spectrom.* **2001**, *12*, 343–347.
30. Null, A. P.; Nepomuceno, A. I.; Muddiman, D. C. Implications of Hydrophobicity and Free Energy of Solvation for Characterization of Nucleic Acids by Electrospray Ionization Mass Spectrometry. *Anal. Chem.* **2003**, *75*, 1331–1339.
31. Cech, N. B.; Enke, C. G. Relating Electrospray Ionization Response to Nonpolar Character of Small Peptides. *Anal. Chem.* **2000**, *72*, 2717–2723.
32. Enke, C. G. A Predictive Model for Matrix and Analyte Effects in Electrospray Ionization of Singly-Charged Ionic Analytes. *Anal. Chem.* **1997**, *69*, 4885–4893.
33. Fenn, J. B. Ion Formation from Charged Droplets: Roles of Geometry, Energy, and Time. *J. Am. Soc. Mass Spectrom.* **1993**, *4*, 524–535.
34. Eaton, W. A.; Henry, E. R.; Hofrichter, J.; Mozzarelli, A. Is Cooperative Oxygen Binding by Hemoglobin Really Understood. *Nat. Struct. Biol.* **1999**, *6*, 351–358.
35. Griffith, W. P.; Kaltashov, I. A. Mass Spectrometry in the Study of Hemoglobin: From Covalent Structure to Higher Order Assembly. *Curr. Org. Chem.* **2006**, *10*, 535–553.
36. Griffith, W. P.; Kaltashov, I. A. Highly Asymmetric Interactions between Globin Chains during Hemoglobin Assembly Revealed by electrospray Ionization Mass Spectrometry. *Biochemistry* **2003**, *42*, 10024–10033.
37. Simmons, D. A.; Wilson, D. J.; Lajoie, G. A.; Doherty-Kirby, A.; Konermann, L. Subunit Disassembly and Unfolding Kinetics of Hemoglobin Studied by Time-resolved Electrospray Mass Spectrometry. *Biochemistry* **2004**, *43*, 14792–14801.
38. Hossain, B. M.; Konermann, L. Pulsed Hydrogen/Deuterium Exchange MS/MS for Studying the Relationship between Noncovalent Protein Complexes in Solution and in the Gas Phase after Electrospray Ionization. *Anal. Chem.* **2006**, *78*, 1613–1619.
39. Rai, D. K.; Landin, B.; Alvelius, G.; Griffiths, W. J. Electrospray Tandem Mass Spectrometry of Intact β-Chain Hemoglobin Variants. *Anal. Chem.* **2002**, *74*, 2097–2102.
40. Griffith, W. P.; Kaltashov, I. A. Protein Conformational Heterogeneity as a Binding Catalyst: ESI-MS Study of Hemoglobin H Formation. *Biochemistry* **2007**, *46*, 2020–2026.
41. Schmidt, A.; Karas, M. The Influence of Electrostatic Interactions on the Detection of Heme-Globin Complexes in ESI-MS. *J. Am. Soc. Mass Spectrom.* **2001**, *12*, 1092–1098.
42. Versluis, C.; Heck, A. J. R. Gas-phase Dissociation of Hemoglobin. *Int. J. Mass Spectrom.* **2001**, *210/211*, 637–649.
43. Mekecha, T. T.; Amunugama, R.; McLuckey, S. A. Ion Trap Collision-induced Dissociation of Human Hemoglobin α-Chain Cations. *J. Am. Soc. Mass Spectrom.* **2006**, *17*, 923–931.
44. Antonini, E.; Brunori, M. Hemoglobin and Myoglobin in Their Reactions With Ligands; North-Holland Publishing Company: Amsterdam, 1971; p 21
45. Glasoe, P. K.; Long, F. A. Use of Glass Electrodes to Measure Acidities in Deuterium Oxide. *J. Am. Chem. Soc.* **1960**, *64*, 188–190.
46. Hossain, B. M.; Simmons, D. A.; Konermann, L. Do Electrospray Mass Spectra Reflect the Ligand Binding State of Proteins in Solution? *Can. J. Chem.* **2005**, *83*, 1953–1960.
47. Kyte, J.; Doolittle, R. A Simple Method for Displaying the Hydropathic Character of a Protein. *J. Mol. Biol.* **1982**, *157*, 105–132.
48. Englander, S. W. Hydrogen Exchange and Mass Spectrometry: A Historical Perspective. *J. Am. Soc. Mass Spectrom.* **2006**, *17*, 1481–1489.
49. Krishna, M. M. G.; Hoang, L.; Lin, Y.; Englander, S. W. Hydrogen Exchange Methods to Study Protein Folding. *Methods* **2004**, *34*, 51–64.
50. Bai, Y.; Milne, J. S.; Mayne, L.; Englander, S. W. Primary Structure Effects on Peptide Group Hydrogen Exchange. *Proteins: Struct. Funct. Genet.* **1993**, *17*, 75–86.
51. Katta, V.; Chait, B. T. Hydrogen/Deuterium Exchange Electrospray Ionization Mass Spectrometry: A Method for Probing Protein Conformational Changes in Solution. *J. Am. Chem. Soc.* **1993**, *115*, 6317–6321.
52. Creighton, T. E. *Proteins*; W. H. Freeman & Co: New York; 1993.
53. Thomson, B. A. Declustering and Fragmentation of Protein Ions from an Electrospray Ion Source. *J. Am. Soc. Mass Spectrom.* **1997**, *8*, 1053–1058.
54. McKay, A. R.; Ruotolo, B. T.; Ilag, L. L.; Robinson, C. V. Mass Measurements of Increased Accuracy Resolve Heterogeneous Populations of Intact Ribosomes. *J. Am. Chem. Soc.* **2006**, *128*, 11433–11442.
55. Frahm, J. L.; Muddiman, D. C.; Burke, M. J. Leveling Response Factors in the Electrospray Ionization Process Using a Heated Capillary Interface. *J. Am. Soc. Mass Spectrom.* **2005**, *16*, 772–778.
56. Wyttenbach, T.; Liu, D.; Bowers, M. T. Hydration of Small Peptides. *Int. J. Mass Spectrom.* **2005**, *240*, 221–232.
57. Wang, W.; Kitova, E. N.; Klassen, J. S. Influence of Solution and Gas Phase Processes on Protein-Carbohydrate Binding Affinities Determined by Nanoelectrospray Fourier Transform Ion Cyclotron Resonance Mass Spectrometry. *Anal. Chem.* **2003**, *75*, 4945–4955.
58. Peschke, M.; Verkerk, U. H.; Kebarle, P. Features of the ESI Mechanism That Affect the Observation of Multiply Charged Noncovalent Protein Complexes and the Determination of the Association Constant by the Titration Method. *J. Am. Soc. Mass Spectrom.* **2004**, *15*, 1424–1434.
59. Tahallah, N.; Pinkse, M.; Maier, C. S.; Heck, A. J. R. The Effect of the Source Pressure on the Abundance of Ions of Noncovalent Protein Assemblies in an Electrospray Ionization Orthogonal Time-of-Flight Instrument. *Rapid Commun. Mass Spectrom.* **2001**, *15*, 596–601.